SUPPLEMENTARY INFORMATION

Jadeite and related species in shocked meteorites: Limitations on inference of shock conditions

Baziotis, I.[1*], Xydous, S.[1], Papoutsa, A.[1], Hu, J.[2], Ma, C.[2], Klemme, S.[3], Berndt, J.[3], Ferrière, L.[4], Caracas, R.[5,6] & Asimow, P. D.[2]

[1]Agricultural University of Athens, Natural Resources Management and agricultural engineering, Laboratory of Mineralogy and Geology, Iera Odos 75, 11855, Athens, Greece; *ibaziotis@aua.gr

[2]California Institute of Technology, Division of Geological and Planetary Sciences, Pasadena, CA 91125, USA

[3]Westfälische Wilhelms-Univ. Münster, Institut für Mineralogie, Correnstrasse 24, 48149 Münster, Germany

[4]Natural History Museum, Burgring 7, A-1010, Vienna, Austria

[5]CNRS, Ecole Normale Supérieure de Lyon, Laboratoire de Géologie de Lyon LGLTPE UMR5276, Centre Blaise Pascal, 46 allée d'Italie Lyon 69364, France

[6]The Center for Earth Evolution and Dynamics (CEED), University of Oslo, Blindern, Oslo, Norway

Supplementary Figures S1-S3

Supplementary References 13

Supplementary Figures

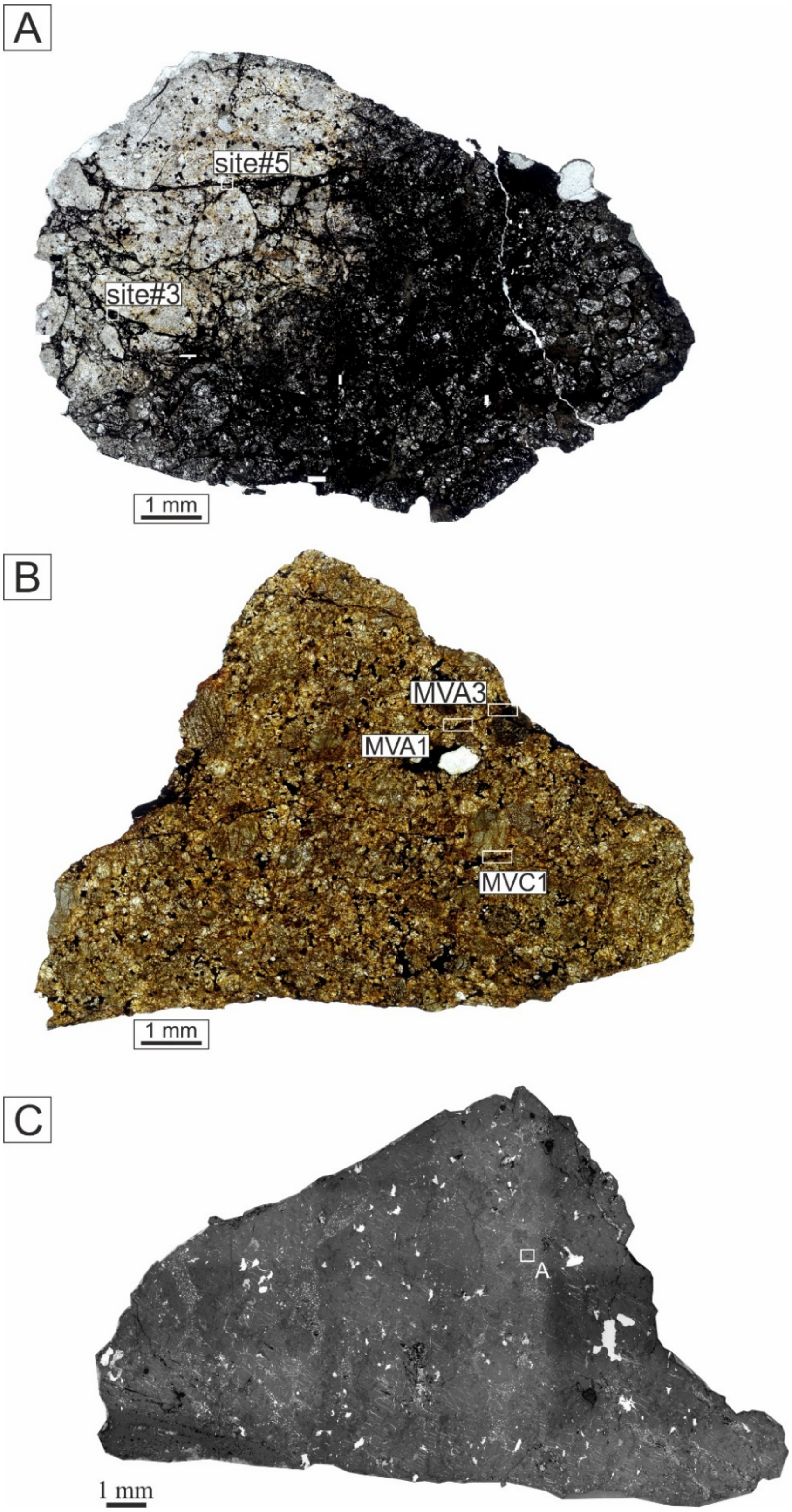

Fig. S1 Photomicrograph mosaics of the studied sections: (A) *Ozerki*, (B) *Chug Chug 011*, and (C) *Chantonnay*, built from transmitted (A and B) or reflected (C) light photographs. Rectangular white frames indicate the areas where high-pressure polymorphs were found; these are enlarged in Figs. 2 and 3 in the main text.

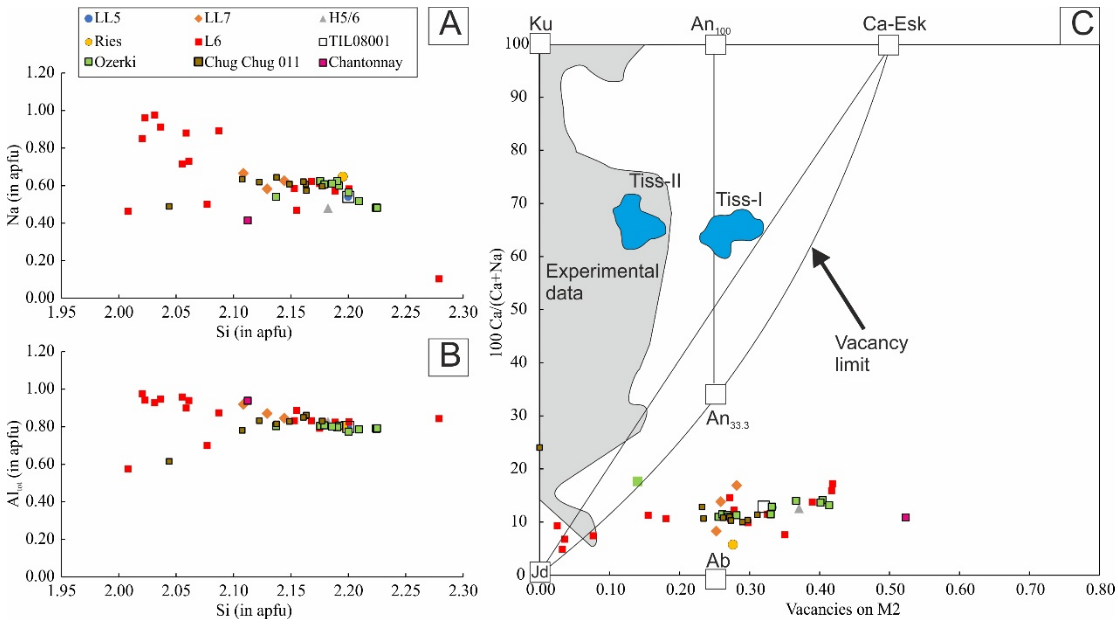

Fig. S2 Compositional data for jadeite and it`s relatives from the literature and this work. Si vs. Na (A) and vs. Al_{tot} (B) for the literature and data from this work. In (C) Ca# [molar Ca/(Ca+Na)] expressed as percent vs. vacancies on M2 site. The compositions of the published work, and of this study are restricted to the portion of the diagram below the curve labeled "vacancy limit," which defines the locus of points for which the M1 site is fully occupied with 3^+ cations and the tetrahedral site by 4^+ cations, and at narrow Ca# range (~10-20). The compositions for plagioclases defined in terms of a clinopyroxene formula unit, plot along a vertical line at an M2 vacancy concentration of 0.25; this line extends from end-member anorthite (Ca# of 100), labeled An_{100}, through a Ca# of 33.3 ($An_{33.3}$)(vacancy limit curve) to the Ca# 0 of albite (Ab). The tissintites (Tiss-I and Tiss-II) are plotted on the locus of points for which the Ca# range is narrow ~60-70; both tissintites represent under-silicic and highly-defective high pressure clinopyroxenes (Ma et al. 2015, 2017). Compositions for jadeite (Jd), kushiroite (Ku), the Ca-Eskola component (Ca-Es), and albite (Ab) are also shown. The gray field encloses data from equilibration and synthesis experiments (Wood and Henderson 1978; Gasparik 1984, 1985, 1986; Irifune et al. 1986; Ono and Yasuda 1986; Pertermann and Hirschmann 2002; Okamoto and Maruyama 2004; Zhao et al. 2011; Ishii et al. 2012; Massonne and Fockenberg 2012; Knapp et al. 2013).

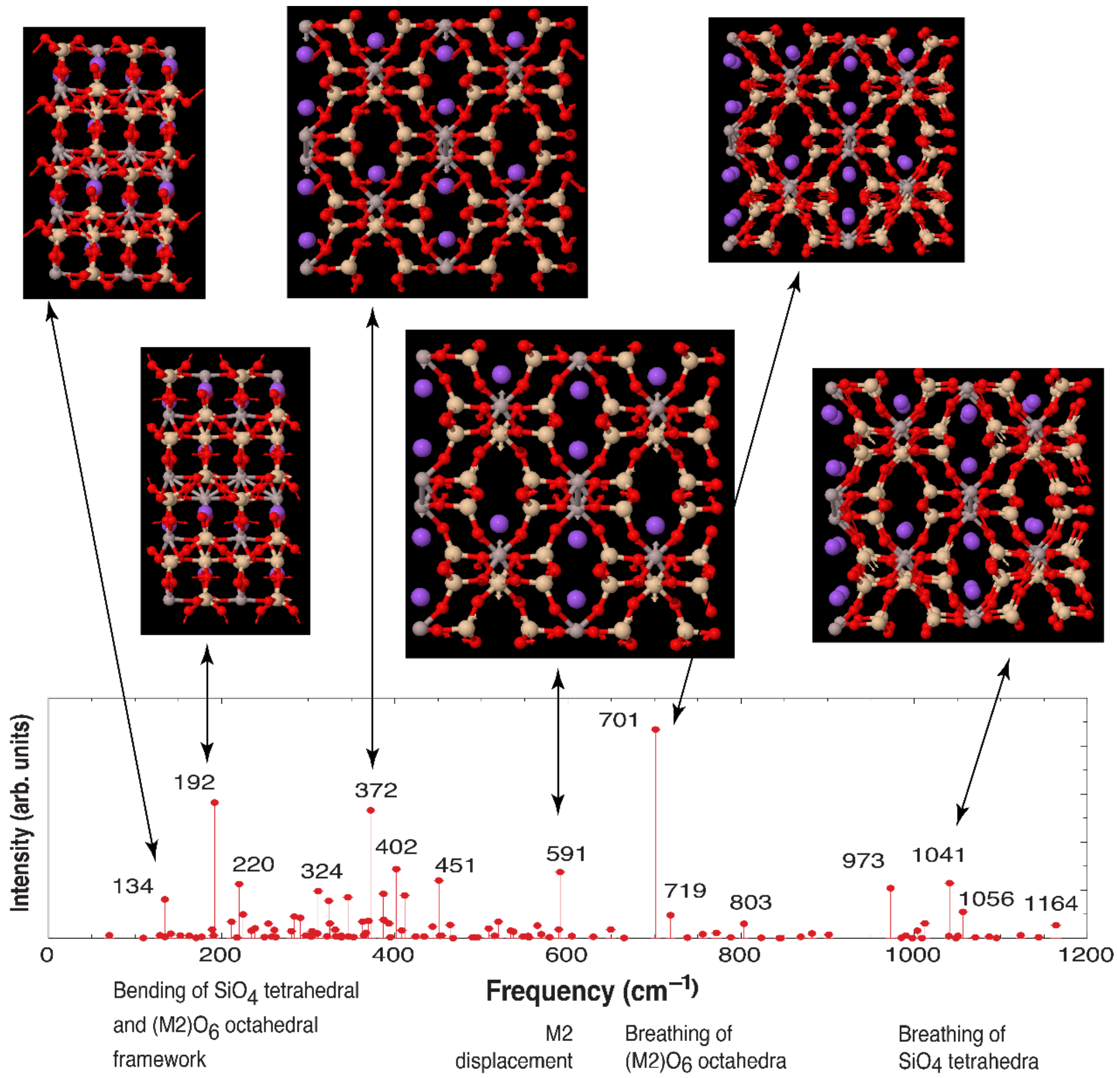

Fig. S3 Vibrational patterns of a few representative modes in the albitic jadeite pyroxene. Na, Al, Si, and O are represented with purple, grey, light brown, and red spheres, respectively. The high-intensity Raman modes are labeled with their frequency (in cm^{-1}). The modes are computed at 0K, hence there is no calculated broadening due to anharmonicity or thermal effects.

Supplementary References

Gasparik, T. (1984) Experimentally determined stability of clinopyroxene+ garnet+corundum in the system CaO–MgO–Al_2O_3–SiO_2. *American Mineralogist* **69**, 1025-1035.

Gasparik, T. (1985) Experimental study of subsolidus phase relations and mixing properties of pyroxene and plagioclase in the system Na_2O-CaO-Al_2O_3-SiO_2. *Contributions to Mineralogy and Petrology* **89**, 346-357.

Gasparik, T. (1986) Experimental study of subsolidus phase relations and mixing properties of clinopyroxene in the silica-saturated system CaO-MgO-Al_2O_3-SiO_2. *American Mineralogist* **71**, 686-693.

Irifune, T., Sekine, T., Ringwood, A.E., & Hibberson, W.O. (1986) The eclogite-garnetite transformation at high pressure and some geophysical implications. *Earth and Planetary Science Letters* **77**, 245-256.

Ishii, T., Kojitani, H., & Akaogi, M. (2012) High-pressure phase transitions and subduction behavior of continental crust at pressure–temperature conditions up to the upper part of the lower mantle. *Earth and Planetary Science Letters* **357**, 31-41.

Knapp, N., Woodland, A. B., & Klimm, K. (2013) Experimental constraints in the CMAS system on the Ca-Eskola content of eclogitic clinopyroxene. *European Journal of Mineralogy* **25**, 579-596.

Ma, C., & Beckett, J.R. (2017) A new type of tissintite, (Ca,Mg,Na,$\square_{0.14}$)(Al,Fe,Mg)Si_2O_6, in the Zagami Martian meteorite: a high-pressure clinopyroxene formed by shock. In Lunar and Planetary Science Conference (No. 1964, p. 1639).

Massonne, H. J., & Fockenberg, T. (2012) Melting of metasedimentary rocks at ultrahigh pressure—Insights from experiments and thermodynamic calculations. *Lithosphere* **4**, 269-285.

Okamoto, K., & Maruyama, S. (2004) The eclogite–garnetite transformation in the MORB+H_2O system. *Physics of the Earth and Planetary Interiors* **146**, 283-296.

Ono, S., & Yasuda, A. (1996) Compositional change of majoritic garnet in a MORB composition from 7 to 17 GPa and 1400 to 1600 C. *Physics of the Earth and Planetary Interiors* **96**, 171-179.

Pertermann, M., & Hirschmann, M.M. (2002) Trace-element partitioning between vacancy-rich eclogitic clinopyroxene and silicate melt. *American Mineralogist* **87**, 1365-1376.

Wood, B.J., & Henderson, C.M.B. (1978) Compositions and unit-cell parameters of synthetic non-stoichiometric tschermakitic clinopyroxenes. *American Mineralogist* **63**, 66-72.

Zhao, S., Nee, P., Green, H.W., & Dobrzhinetskaya, L.F. (2011) Ca-Eskola component in clinopyroxene: Experimental studies at high pressures and high temperatures in multianvil apparatus. *Earth and Planetary Science Letters* **307**, 517-524.